NASA CONTRACTOR REPORT

NASA CR-1631

XB-70 FLIGHT TEST DATA COMPARISONS WITH SIMULATION PREDICTIONS OF INLET UNSTART AND BUZZ

by Arnold W. Martin and Warren D. Beaulieu

Prepared by
NORTH AMERICAN ROCKWELL CORPORATION
Los Angeles, Calif.
for Flight Research Center

NATIONAL AERONAUTICS AND SPACE ADMINISTRATION • WASHINGTON, D. C. • JUNE 1970

1. Report No. NASA CR-1631	2. Government Accession No.	3. Recipient's Catalog No.
4. Title and Subtitle XB-70 FLIGHT TEST DATA COMPARISONS WITH SIMULATION PREDICTIONS OF INLET UNSTART AND BUZZ		5. Report Date June 1970 6. Performing Organization Code
7. Author(s) Arnold W. Martin and Warren D. Beaulieu		8. Performing Organization Report No. 10. Work Unit No.
9. Performing Organization Name and Address North American Rockwell Corporation Los Angeles Division Los Angeles, California		11. Contract or Grant No. NAS4-1175 13. Type of Report and Period Covered Contractor Report
12. Sponsoring Agency Name and Address NATIONAL AERONAUTICS AND SPACE ADMINISTRATION Washington, D. C. 20546		14. Sponsoring Agency Code

15. Supplementary Notes

16. Abstract

Comparisons have been made of XB-70 flight test data and simulation runs for three propulsion system transients. The three transients were (1) a bypass-closing-induced inlet unstart at a flight Mach number of 2.34, (2) a throat-closing-induced inlet unstart at Mach 2.43, and (3) a throat-opening-induced inlet unstart at Mach 2.43.

The simulation logic and computer program described in NASA CR-928 and NASA CR-73113 were used for the simulation runs. The engines were simulated using the E-30 version of the General Electric Company's simulation program for the YJ-93 engine.

With minor exceptions, the simulation results were in good agreement with the flight test data.

1. Engine Inlets
2. Propulsion Systems

17. Key Words Suggested by Author(s)	18. Distribution Statement
Atmospheric turbulence - Propulsion system - Inlet unstarts - Inlet buzz	Unclassified - Unlimited

19. Security Classif. (of this report)	20. Security Classif. (of this page)	21. No. of Pages	22. Price*
Unclassified	Unclassified	28	$3.00

*For sale by the Clearinghouse for Federal Scientific and Technical Information, Springfield, Virginia 22151

TABLE OF CONTENTS

LIST OF ILLUSTRATIONS

LIST OF SYMBOLS

Symbol	Description	Units
$A_{T_{ef}}/A_{T_{geo}}$	ratio of the effective throat area to the actual geometric throat area	
M	local Mach number	
M_o	freestream Mach number	
P_d	duct average static pressure	psf
P_{tx}	total pressure immediately upstream of the terminal shock	psf
P_{ty}	total pressure immediately downstream of the terminal shock	psf
P_{to}	freestream total pressure	psf
P_{t2}	engine face total pressure	psf or psi
P_y	static pressure immediately downstream of the terminal shock	psf
P_o	freestream static pressure	psf
P_{1407}	static pressure in the duct at FS 1407	psf
$t=0$	time when a simulation run was initiated	
α_o	aircraft angle of attack	degrees
ϵ_y	subsonic diffuser total pressure loss coefficient, $\epsilon_y = (P_{ty} - P_{t2})/(P_{ty} - P_y)$	
ψ_o	aircraft angle of yaw	degrees

XB-70 FLIGHT TEST DATA COMPARISONS WITH SIMULATION PREDICTIONS OF INLET UNSTART AND BUZZ

By Arnold W. Martin and Warren D. Beaulieu

Los Angeles Division of
NORTH AMERICAN ROCKWELL CORPORATION
Los Angeles, California

SUMMARY

Comparisons have been made of XB-70 flight test data and simulation runs for three propulsion system transients. The three transients were (1) a bypass-closing-induced inlet unstart at a flight Mach number of 2.34, (2) a throat-closing-induced inlet unstart at Mach 2.43, and (3) a throat-opening-induced inlet unstart at Mach 2.43.

The simulation logic and computer program described in NASA CR-928 and NASA CR-73113 were used for the simulation runs. The engines were simulated using the E-30 version of the General Electric Company's simulation program for the YJ-93 engine.

With minor exceptions, the simulation results were in good agreement with the flight test data.

INTRODUCTION

The design of a high performance air-breathing propulsion system almost inevitably requires a compromise between steady-state performance and system stability. If stability margins are excessive, performance is sacrificed. If stability margins are inadequate, the consequences can range from inconvenience to loss of an aircraft.

To assist in optimizing the design of the B-70, a digital computer program for simulating propulsion system transient operation was developed cooperatively by the General Electric Company and the North American

Rockwell Corporation. The simulation theory and equations for the air induction system (based on conservation of mass, momentum and energy, and boundary layer separation characteristics determined in wind tunnel model tests) are presented in reference 1. Use of the propulsion system simulation program is discussed in reference 2.

Because the B-70 was designed for Mach 3.0 cruise, the initial use of the simulation program was largely restricted to the 2.6 to 3.0 Mach number range. One of the objectives of the XB-70 flight test program conducted by the NASA Flight Research Center was to evaluate the simulation program at intermediate Mach numbers. Interestingly, accurate simulation of inlet transients is more difficult at intermediate Mach numbers than at high Mach numbers for reasons which include the following:

(1) Operation is near the normal transition between internal-external and all external shock compression. Consequently, the flight test transients are not as sharply defined as are those at higher Mach numbers.

(2) The inlet contraction ratio is small, making the aerodynamic throat location highly sensitive to structural deflections, contour discrepancies, boundary layer bleed distribution, and local flow separation.

(3) The cowl Mach number is such that it is marginal as to whether expulsion of a normal shock will cause boundary layer separation. Where boundary layer separation occurs, the magnitude of the separation is more variable than at higher Mach numbers.

In this investigation, three flight test events were selected by the NASA Flight Research Center for evaluating the simulation results. These were (1) an inlet unstart at Mach 2.34 induced by reducing the bypass area, (2) an inlet unstart at Mach 2.43 induced by reducing the throat area, and (3) an inlet unstart induced by increasing the throat area.

PROCEDURES

Manual inputs to the air induction control system were used to induce the flight test propulsion system transients. For consistency with this procedure, flight test values of bypass area, throat area, throttle position, aircraft Mach number, angle of attack, angle of yaw, and ambient pressure

and temperature were input to the simulation program as functions of time.

To save computer time, preliminary runs to check the validity of the input tables at intermediate Mach numbers were made using a highly simplified engine representation. Input table values which were not included in reference 2 or which were changed as the result of the check runs are listed in the appendix. Following the preliminary checks, each simulation run was repeated using the General Electric Company's E-30 simulation of the YJ-93 engine. Simulation results were then compared to the flight test data.

RESULTS AND DISCUSSION

Inlet Unstart Induced by Closing the Bypass

Flight test transient. - The bypass-induced inlet unstart selected for simulation occurred on flight 78 of XB-70 Ship 1. At a flight Mach number of 2.34, an altitude of 56,180 feet and an angle of attack of 3.5 degrees, a transition from manual bypass control to automatic control resulted in a high-rate closing of the bypass doors as shown in the upper portion of figure 1. The flight test instrumentation further showed a coincidental change in sideslip angle from -1 degree to -1.5 degrees (+1 degree to +1.5 degrees yaw). The changes in bypass area and angle of sideslip caused the left inlet to unstart, as evidenced by the engine face total pressure trace of figure 1. Figure 1 also shows that the inlet unstart occurred nearly 0.2 seconds after the bypass area reached its minimum value, suggesting that conditions were marginal as to whether the inlet would unstart. There was no indication of even momentary stall of any of the engines. The right inlet remained started.

Simulation results. - The simulation run was made with the bypass area and yaw angle inputs shown in figure 2. The variation of bypass door area with time was computed using the flight test measurements of the bypass door angles and a calibration test curve of effective flow area versus door angle. The yaw angle input to the simulation program as a function of time was identical to the flight test measurement.

Simulation values of engine face total pressure, terminal shock position, compressor discharge pressure, compressor rotor speed, and engine face total temperature are compared with flight test data in figure 3. For convenience, the flight test data, such as the total pressure trace of

figure 1, have been smoothed prior to replotting. The engine face total temperature data have been amplitude-corrected but not phase-shift-corrected in accordance with the estimated dynamic response characteristics of the high response thermocouple.

Four conceptual diagrams (figure 4) illustrate the modes of inlet operation during the transient. The circled numbers relate the normal shock positions of figure 4 to the engine face total pressure trace of figure 1.

Figure 4(a) illustrates the started mode of inlet operation. The terminal shock is initially at position 1. Simulation and test values at the initiation of the transient are in good agreement as can be seen in the following table:

	Flight	Simulation
Engine face total pressure (psf)	2060	2050
Bypass airflow (lb/sec)	112	109
Engine + secondary airflow (lb/sec)	515	509
Terminal shock position (in.)	1350 $\pm$ 10	1340

With the bypass area decreasing and the captured flow increasing (because of the change in sideslip angle), inflow to the duct exceeds outflow, engine face total pressure rises and the terminal shock wave moves upstream.

After the terminal shock has moved upstream of the aerodynamic throat (shock position 2 in figure 4(b)) continuity relationships drive the terminal shock toward the cowl lip. This unstarting phase is terminated as the shock passes forward of the cowl lip.

Figure 4(c) illustrates the emptying phase of the unstart cycle. As the terminal shock moves upstream past the cowl lip to position 3u, the pressure rise across the shock causes massive boundary layer separation. With the effective throat area reduced by the separated boundary layer, outflow from the duct exceeds inflow through the choked throat. A new terminal shock, 3, forms at the effective throat and moves downstream as required to match the airflow supply and demand. (Note there is both an external normal shock and an internal terminal shock in this mode of operation.)

Model and flight test data for the B-70 and other inlet configurations have shown that the magnitude of the boundary layer separation will vary somewhat from incident to incident over a range that is dependent on the cowl lip Mach number (the static pressure rise across the terminal shock). Based on comparisons of model test data and simulation results (see the appendix) the boundary layer separation for this flight condition was assumed to reduce the effective throat area to 60 percent of the geometric area. Increased or decreased amounts of separation will increase or decrease the rate of engine face pressure drop during the emptying phase.

With inflow restricted by the boundary layer separation in the throat region, duct pressure drops to the point where reattachment of the boundary layer occurs. In this simulation run reattachment was initiated at a P_d/P_o (ratio of duct static to ambient pressure) value of 9. Analysis of data for many unstart and buzz cycles and several configurations has shown that the reattachment pressure ratio, P_d/P_o, varies from incident to incident as well as from configuration to configuration. However, P_d/P_o for reattachment falls into a rather consistent band ranging from approximately 4 for severe unstart and buzz cycles to approximately 11 for mild cycles. While the probability of severe cycles is greater at high Mach numbers, mild cycles at high Mach numbers and severe cycles at lower Mach numbers have been observed on occasion.

At the time of boundary layer reattachment, pressure in the duct is low and flow in the throat is sonic. Outflow, proportional to the engine face total pressure, is initially low. With inflow exceeding outflow, mass and pressure in the duct increase and the terminal shock (figure 4(c)) moves forward. Depending on the effective throat area and the corrected airflow demand of the engine and bypass systems, the terminal shock will either reach a stable unstarted supercritical operating point or continue forward and out of the inlet. In the latter event, if the static pressure ratio across the terminal shock is sufficiently high, the throat region boundary layer will again separate and a new buzz cycle will be initiated. The simulation program predicted that a new buzz cycle would be initiated. The test data suggest that, as the terminal shock moved upstream of the throat, a small separation of the throat region boundary layer occurred. This separation reduced the inflow sufficiently to result in marginally stable unstarted supercritical operation. Note that the bypass area was increasing during this portion of the transient as shown in figure 1.

Both the flight test data and the simulation predictions indicate that

the inlet pressure transients were not sufficient to cause even momentary compressor stall.

Inlet Unstart Induced by Reducing Throat Area

Flight test transient. - Inlet unstart was induced in flight 68 by manually reducing the throat area of the left inlet. Flight conditions immediately prior to the transient were as follows:

Mach number	2.43
Altitude	57,580 ft
Angle of attack	3.6 deg
Angle of sideslip	0
Total pressure recovery	.81
Throttle setting	77 deg (partial afterburner)

The inlet was operating nearly 15 percent supercritically with the terminal shock well downstream of the throat.

Figure 5 presents oscillograph traces of an engine face total pressure and a duct wall static pressure at fuselage station (FS) 1407. These and additional wall static pressure traces show that as the throat area was decreased, the terminal shock first moved aft. As the throat closed further, a second normal shock formed at the effective throat and proceeded forward to the cowl lip. The terminal shock moved upstream momentarily as the inlet unstarted, then returned to essentially its original position. That is, the terminal shock remained downstream of the inlet throat throughout the transition from started to unstarted supercritical operation. Inlet operation was sufficiently supercritical throughout the transient to prevent massive separation of the boundary layer. Consequently, there was no "emptying phase" during the unstart and the engine face total pressure transient was relatively small. Engine operation was normal throughout the transient.

Simulation results. - The flight test rate of change of throat area was such that the unstart was not induced for several seconds. To reduce computer costs, the rate of throat area decrease was increased for the simulation. Because the rate of closing was still slow relative to the system dynamics, the primary effect was to change the time scale in the initial part of the transient. The throat area change input to the simulation is shown in figure 6.

The diagram of figure 7 serves to illustrate the various events in the simulation transient.

Prior to the transient, the terminal shock is at position 1, figure 7(a). As the throat closes, both the airflow captured by the inlet and the corrected airflow demand of the engine and bypass systems remain constant. Consequently, the terminal shock moves aft, position 2, to maintain the same total pressure recovery. (Inasmuch as the throat area change has little effect on either the total pressure losses through the oblique shock system or the total flow at the shock station, the terminal shock will move to maintain the same area and, therefore, Mach number just upstream of the shock station.)

As the throat area continues to decrease, throat Mach number approaches unity. With further reduction, the throat area can no longer pass all the flow captured by the inlet. With inflow to the throat exceeding outflow, a normal shock forms, position 3u of figure 7(b), and moves upstream past the cowl lip, position 4u. As inflow and total pressure recovery at the upstream face of the terminal shock decrease, the terminal shock also moves upstream, from position 3 to 4.

Because of the highly supercritical operation at the initiation of the throat-closing transient, flow in and immediately downstream of the throat is sonic or supersonic throughout the transient. Thus the duct static pressure in this region relative to ambient pressure is below the simulation criterion for initiating boundary layer reattachment. Therefore, the boundary layer does not separate as the upstream normal shock moves forward of the cowl lip. Following expulsion of the upstream normal shock, the pressure recovery and flow stabilize at the lower values associated with the external normal shock total pressure loss. During this stabilizing period, the terminal shock moves aft to a position similar to its position when the throat flow first became sonic.

While the flight test instrumentation was not sufficient to completely define the terminal shock travel and the formation and travel of the upstream normal shock, the simulation program and the flight test data are generally in good agreement.

The following table compares several flight test and simulation parameters at the initiation of the transient.

	Flight	Simulation
Engine face total pressure (psf)	2080	2100
Bypass airflow (lb/sec)	98	100
Engine + secondary airflow (lb/sec)	507	509
Terminal shock position (in.)	1405 $\pm$ 3	1405

Figure 8 shows the correlation between the flight test static pressure trace at FS 1407 and the simulation values of terminal shock position versus time. Initially, the terminal shock is slightly upstream of FS 1407. Consequently, flow is subsonic and the static pressure is relatively high. As the throat closes, area at FS 1407 decreases. With essentially constant total pressure and flow quantity, the subsonic Mach number increases and the local static pressure decreases. As the throat continues to close, the terminal shock moves downstream of the pressure tap at FS 1407. The local flow is then supersonic, and the static pressure drops. (Note the time scale change because of the higher rate of throat area change for the simulation run.) As the upstream normal shock forms and moves out of the inlet, the terminal shock moves upstream and crosses the static pressure tap at FS 1407. Static pressure jumps as the local flow becomes subsonic, then drops again as the inlet stabilizes in supercritical unstarted operation with the terminal shock aft of FS 1407. During this portion of the transient, the inlet dynamics rather than the throat closing rate are controlling. Thus the higher rate of area change for the simulation run has little effect on the time scales for this portion of the transient.

Additional simulation and flight test parameters are presented in figure 9.

The major discrepancy between the flight test and simulation data is that the flight test static pressure instrumentation indicated that the "upstream" normal shock formed well aft of the nominal geometric throat station. The unexpectedly far aft position may be the result of either or a combination of two factors, local boundary layer separation, and a difference between the actual throat geometry and that computed from the simulation input table of area versus station. At this flight Mach number, the area-versus-station curve is fairly flat and somewhat discontinuous because of the ramp hinge mechanism. Consequently rather small deviations of the actual geometry from the simulation table values can change the effective aerodynamic throat location. Dimensional checks of the inlet

at the maximum and minimum throat area settings showed good agreement with the simulation tables; however, no dimensional checks were made at the intermediate throat areas of this transient.

The initial check run with the simplified engine representation gave higher rates of pressure drop during the unstarting phase than were observed during the flight. A subsequent check run wherein the area-versus-station curves were arbitrarily changed (area was reduced as shown in figure 10) gave engine face total pressure rates of change more in agreement with the flight test data. Consequently, the modified area table was used in the final simulation run with the General Electric E30 engine representation. Figure 10 compares the engine face total pressure histories computed with the design area table and with the modified area table.

In summary, the discrepancies between the simulation results and the flight data indicate (1) the effective throat is aft of the design geometry location and (2) the rate of area change with station between the effective throat and cowl lip is less than the design geometry value. Both differences could be caused by local boundary layer separation and/or differences between the actual and design geometry.

Inlet Unstart Induced by Increasing Throat Area

Flight test transient. - A throat-opening-induced unstart on flight 68 was initiated at Mach 2.43 at an altitude of 58,080 feet and an angle of attack of 3.7 degrees. Average engine face total pressure recovery prior to the unstart was .88. The unstart pressure variation during the unstart and subsequent mild buzz is illustrated in the oscillograph trace of figure 11. Engine operation was normal during the transient.

Simulation results. - The throat area variation with time input to the simulation program is presented in figure 12. The time required for the change was reduced by approximately 50 percent from the flight test values to reduce computer run times.

The simulation transient is illustrated by the diagrams of figure 13. As the throat begins to open, the terminal shock moves upstream as shown in figure 13(a). The shock moves to maintain essentially a constant area and Mach number at its upstream face inasmuch as there is negligible change in the captured airflow quantity, and the corrected airflow demands of the

engine and bypass systems have not changed. Eventually the throat opens to the extent that the terminal shock moves forward of the aerodynamic throat. The terminal shock then accelerates as it moves upstream toward the cowl lip (figure 13(b)). As the terminal shock moves out of the inlet, the static pressure rise causes massive boundary layer separation in the inlet. The subsequent emptying cycle is illustrated in figure 13(c). With inflow restricted, duct pressure decreases to the level where the separated boundary layer reattaches. Inflow then exceeds outflow; mass and pressure in the duct increase; and the terminal shock moves upstream past the throat and to the cowl lip (figure 13(d)). As the terminal shock moves out of the inlet to merge with the external normal shock, the boundary layer separates and a new cycle (buzz) is initiated.

The simulation values and flight test values at the initiation of the unstart were as follows:

	Flight	Simulation
Engine face total pressure (psf)	2190	2135
Bypass airflow (lb/sec)	41	70
Engine + secondary airflow (lb/sec)	545	511
Terminal shock position (in.)	1320	1325

Upon initiation of the simulation run, the program immediately switched from the started to the unstarting phase, indicating that the inlet would not remain started at the specified initial geometry and operating conditions. A subsequent check of the flight test data strongly suggested that the inlet had already entered the unstarting phase at the time selected for t = 0.

Flight test and simulation parameters are presented for comparison in figure 14. Here, as in the throat-closing-unstart simulation using the design inlet geometry, the simulation unstart pressure transient is more severe during the terminal shock travel out of the convergent portion of the inlet. The delayed and sharper total temperature rise at the engine face for the simulation run is consistent with the pressure transient.

The above discrepancies are identical to those of the throat-closing unstart, and can be attributed to local boundary layer separation and/or actual duct geometry differences from the simulation input tables.

In both the throat-closing and throat-opening unstarts, flight test and simulation data would have been in closer agreement had not the simulation rate of throat area change been increased to reduce computing time. However it is believed that the critical portions of the transients were relatively unaffected by the rate change.

CONCLUSIONS

The simulation results are in good agreement with the flight test data, particularly with respect to qualitative predictions. Observed differences are associated primarily with the empirically determined boundary layer separation characteristics during unstart and buzz. The magnitude of these differences is similar to that of the differences observed from one similar event to another in flight tests and model tests.

The simulation program assumes boundary layer separation to be initiated during the unstart cycle only upon expulsion of the terminal shock. The pressure drop and temperature rise characteristics observed in these and other tests suggest that boundary layer separation is initiated as the terminal shock approaches the throat. Such a modification to the assumed boundary layer separation characteristics would moderate the pressure and temperature transients predicted by the simulation program, making them generally more consistent with the observed transients. The existing separation criteria are, however, simpler, more conservative, and in agreement with the more severe transients that have been observed.

The comparison of flight test data and simulation predictions of engine face total temperature during unstart and buzz are considered particularly significant because of the previous lack of such test data. The temperature instrumentation, while excellent by conventional flight test standards, was still inadequate to follow the flight test transients without somewhat questionable analytic corrections for the dynamic characteristics; and, the phase differences between flight and simulation temperature transients are larger than can be readily explained. Nonetheless, the data clearly show that inlet transients such as unstart and buzz are accompanied by appreciable changes in total temperature as predicted by the simulation program.

Los Angeles Division
North American Rockwell Corporation
Los Angeles, California August 20, 1969

APPENDIX

SIMULATION INPUT TABLES

The simulation program requires certain input tables and constants based on empirical data. Reference 2 lists input tables and constants as determined from model tests of the XB-70, with primary emphasis on the Mach 2.6 to 3.0 range. This appendix lists those inputs which have been changed from those of reference 2 after comparison of the flight test data with preliminary simulation runs.

P_{tx}/P_{to} Tables

The tables of total pressure recovery upstream of the terminal shock, P_{tx}/P_{to}, were reduced from the reference 2 values by 2 percent for the started and unstarting phases and by 5 percent for the unstarted phase.

Empirical Constants

The effective throat area during unstarted supercritical inlet operation without boundary layer separation (filling phase) was assumed to be 96 percent of the geometric area.

The effective throat area with massive boundary layer separation (emptying phase) was assumed to be 60 percent of the geometric area. This contrasts with an effective throat area of 5 percent of the geometric area found to be appropriate for Mach 3 operation. Where model test data for a specific configuration is lacking, it is suggested that the following variation of effective throat area with cowl Mach number be assumed.

M_{cowl}	A_{Tef}/A_{Tgeo}
< 1.5	0.96
1.5 to 2.2	linear variation from 0.96 to 0.05
> 2.2	0.05

Reattachment of the boundary layer in the emptying phase is initiated when P_d/P_o, the ratio of duct static to ambient pressure drops below a specified value. As discussed in the body of this report, analysis of a number of model test unstart and buzz cycles indicated that the P_d/P_o value for reattachment varies between 4 and 11 with the probability of the more severe unstart and buzz cycles (low P_d/P_o for reattachment) increasing with increasing flight Mach number. P_d/P_o values of 9 and 11, respectively, gave the best agreement with the test data for the bypass-induced unstart and the throat-increasing unstart of this investigation. A linear variation of P_d/P_o from 4 at freestream Mach number 3 to 10 at Mach 2.4 is suggested for general usage. However, simulation runs to determine the most severe probable unstart and buzz cycles should use a P_d/P_o value of 4.

A subsonic diffuser pressure loss coefficient, ϵ_y, of 0.2 was assumed where

$$\epsilon_y = \frac{P_{ty} - P_{t2}}{P_{ty} - P_y}$$

REFERENCES

1. Martin, Arnold W.: Propulsion System Dynamic Simulation Theory and Equations. North American Aviation, Inc. NASA CR-928, 1968.

2. Martin, Arnold W.; and Wong, Heeman W.: Propulsion System Dynamic Simulation User's Manual. North American Aviation, Inc. (NASA CR-73113), 1967.

M_o = 2.34
Altitude = 56,180 feet
α_o = 3.5°
ψ_o = 0°
P_{t2}/P_{to} = .86

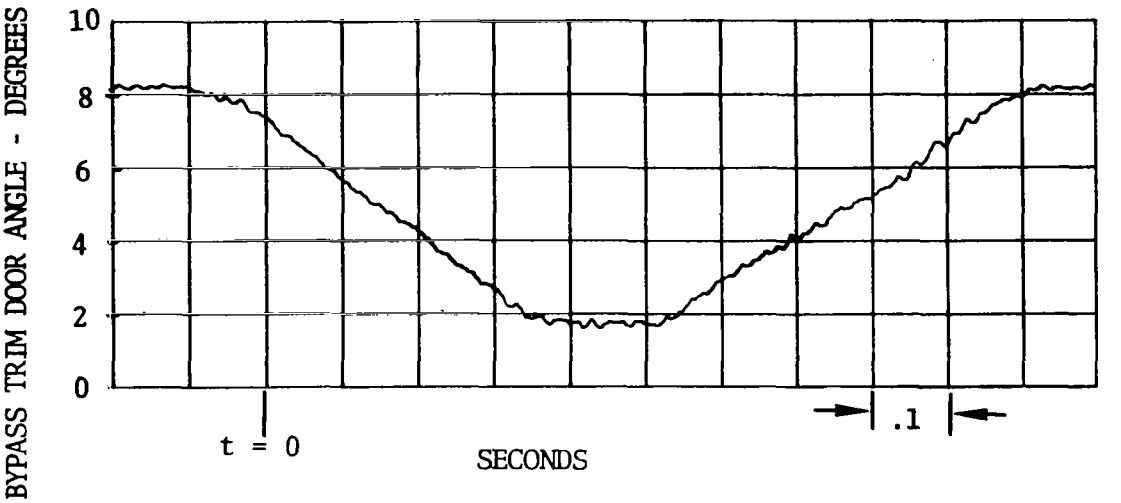

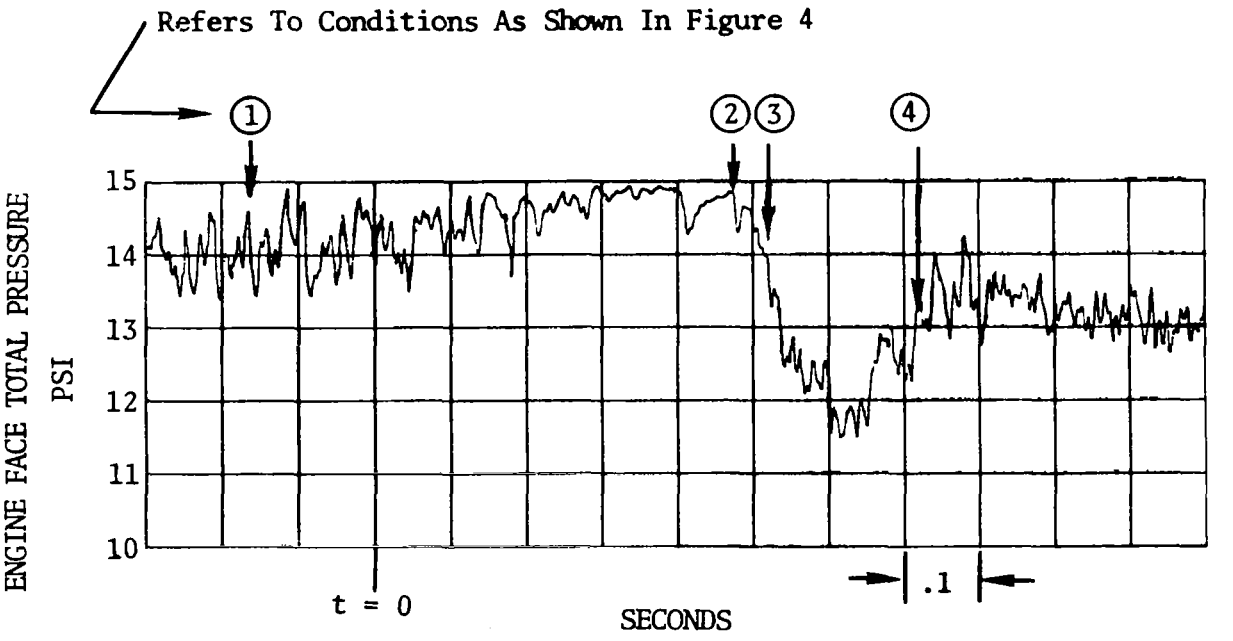

Figure 1. Bypass trim door and engine face total pressure histories for bypass-induced unstart.

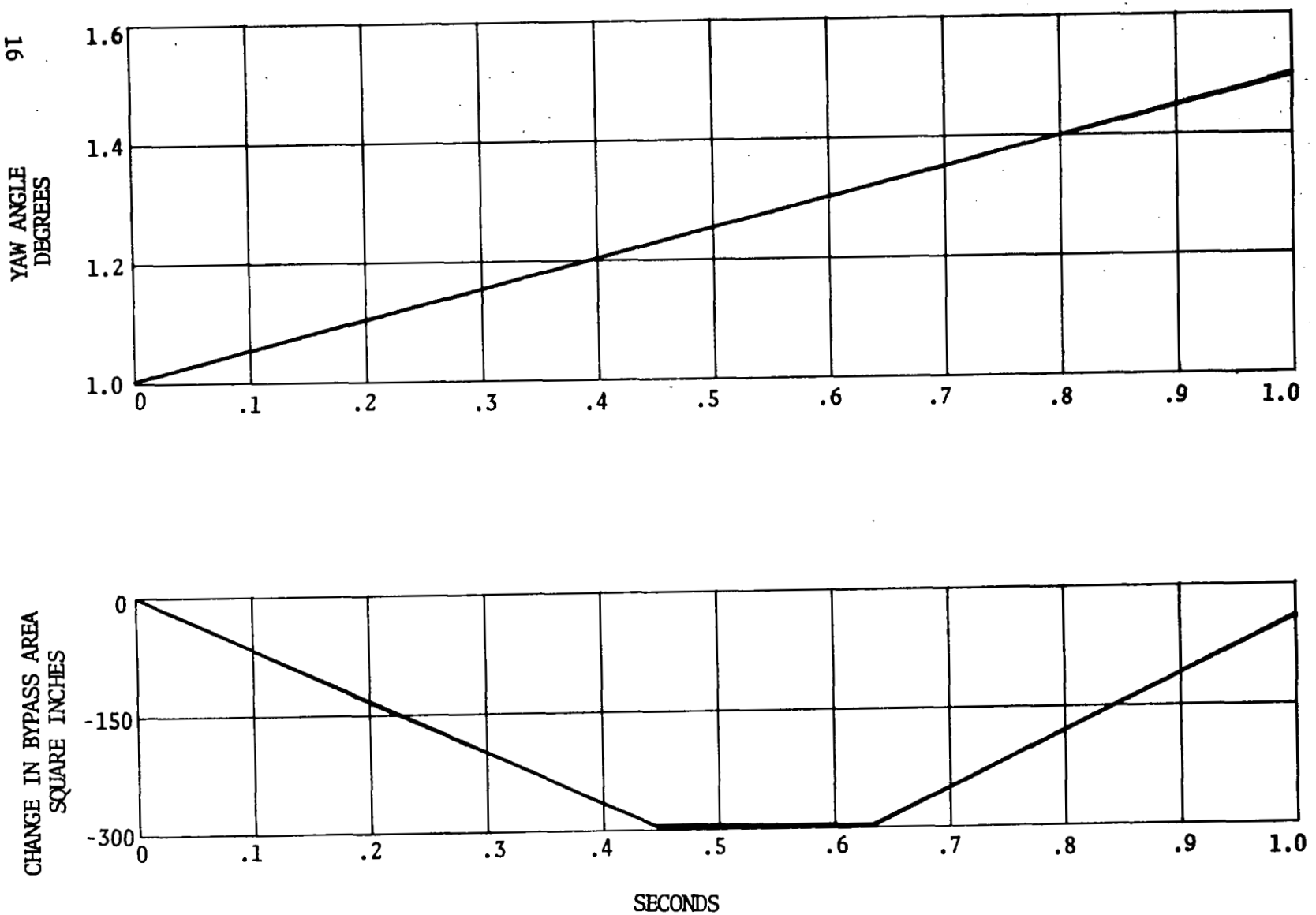

Figure 2. Yaw and bypass area used in simulation for bypass-induced unstart.

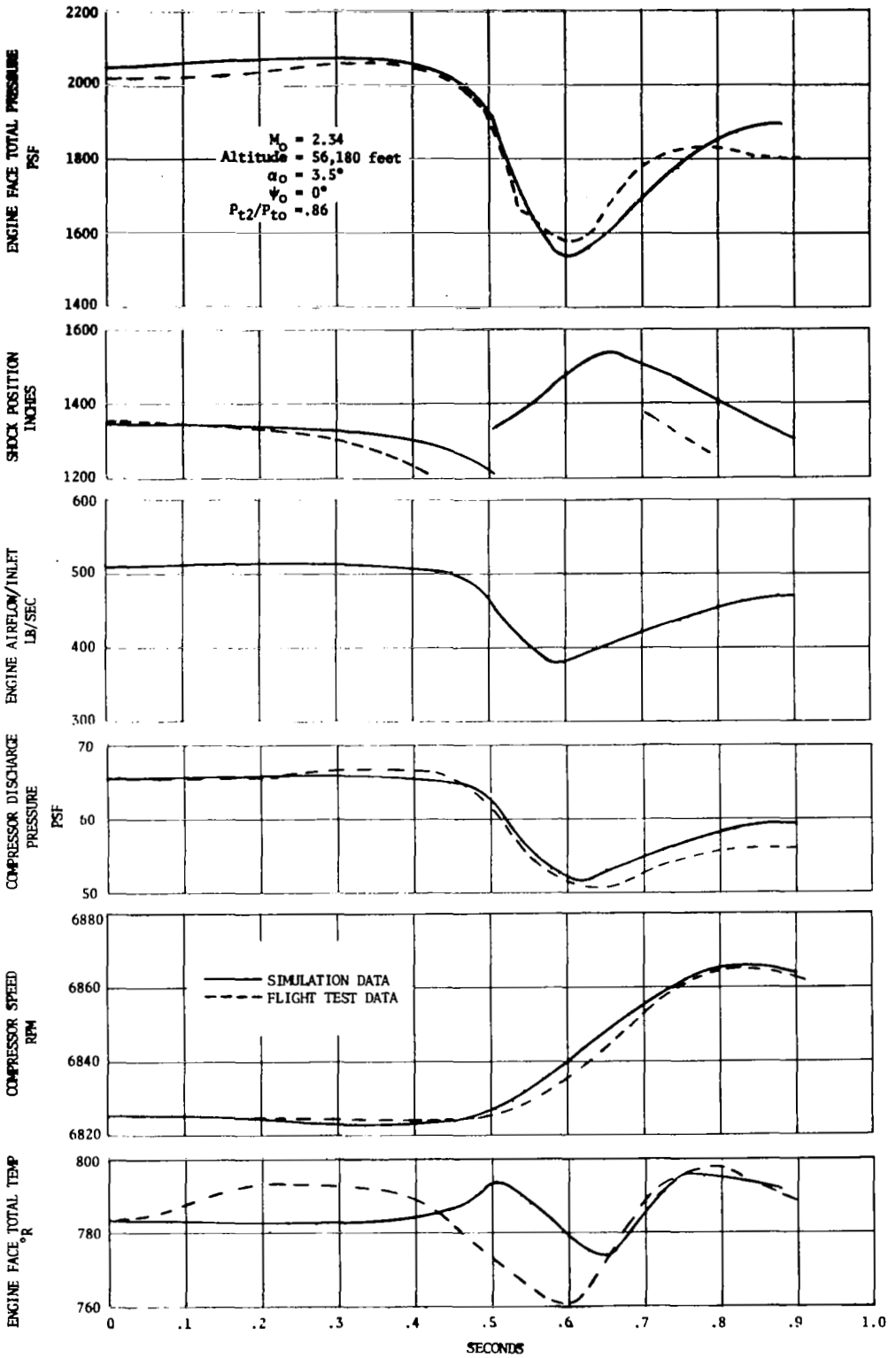

Figure 3. Comparison of flight test data and simulation data for bypass-induced unstart.

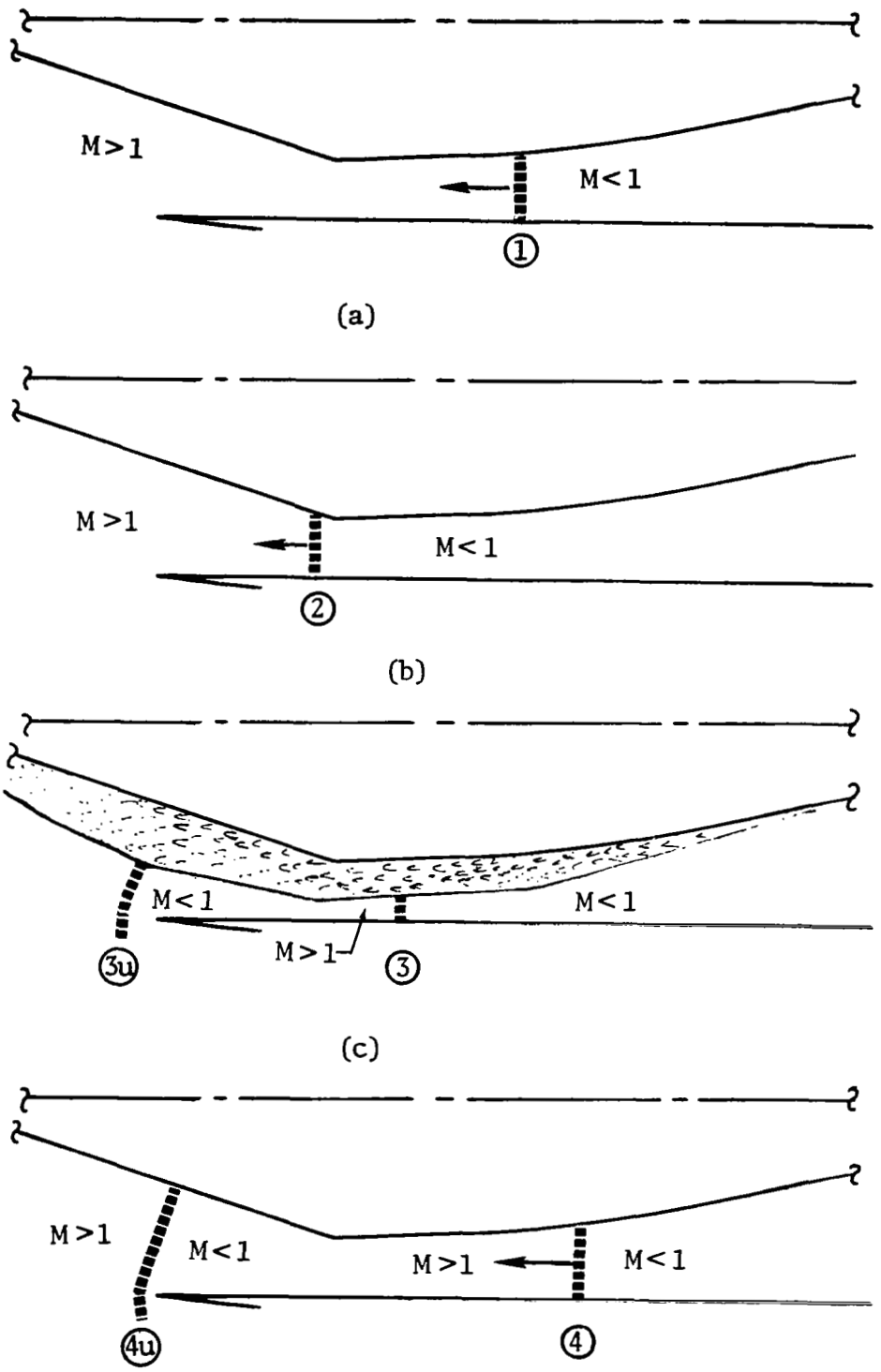

Figure 4. Conceptual diagrams of inlet operation during bypass-induced unstart.

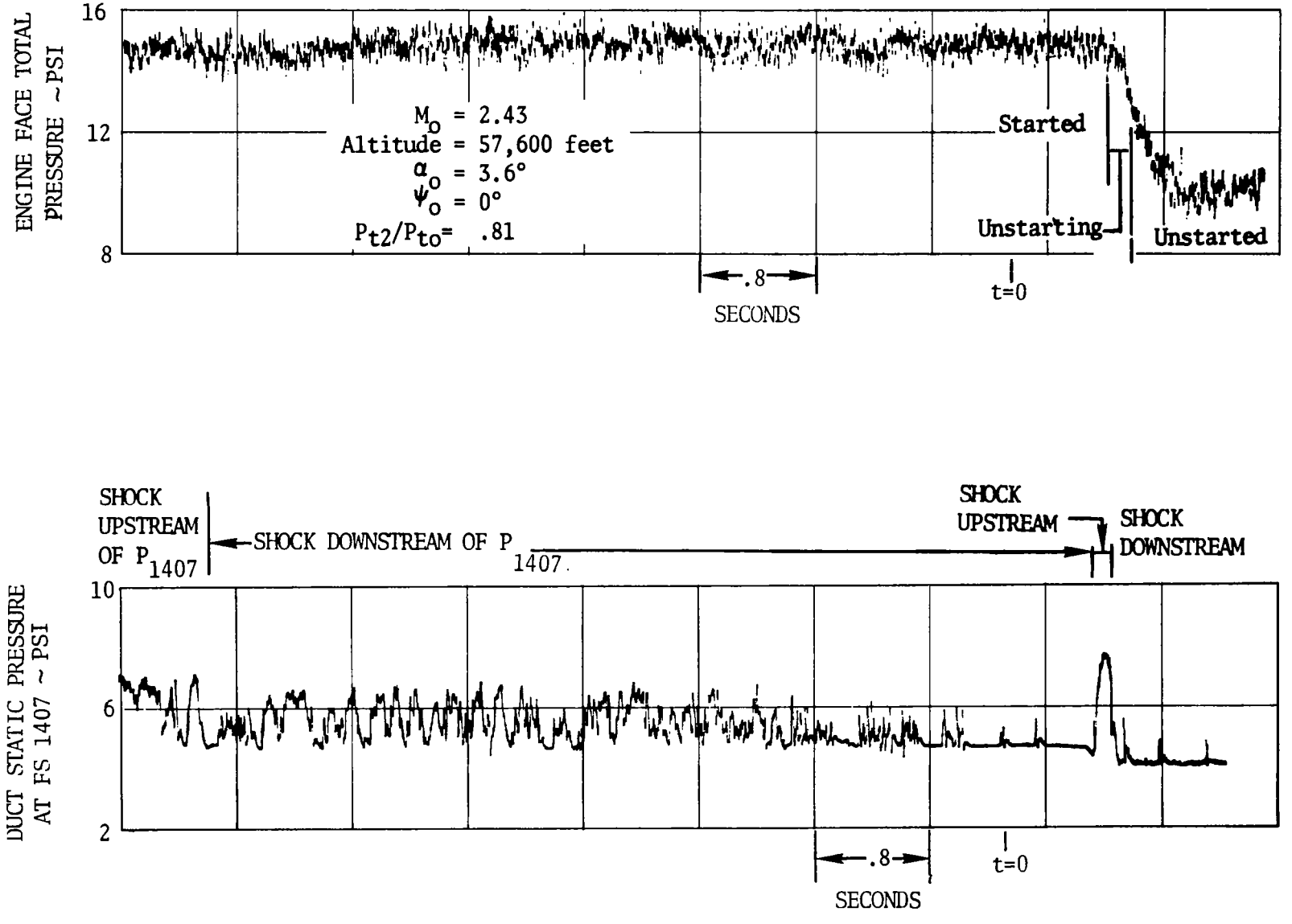

Figure 5. Engine face total pressure and duct wall static pressure histories for throat-decreasing-induced unstart.

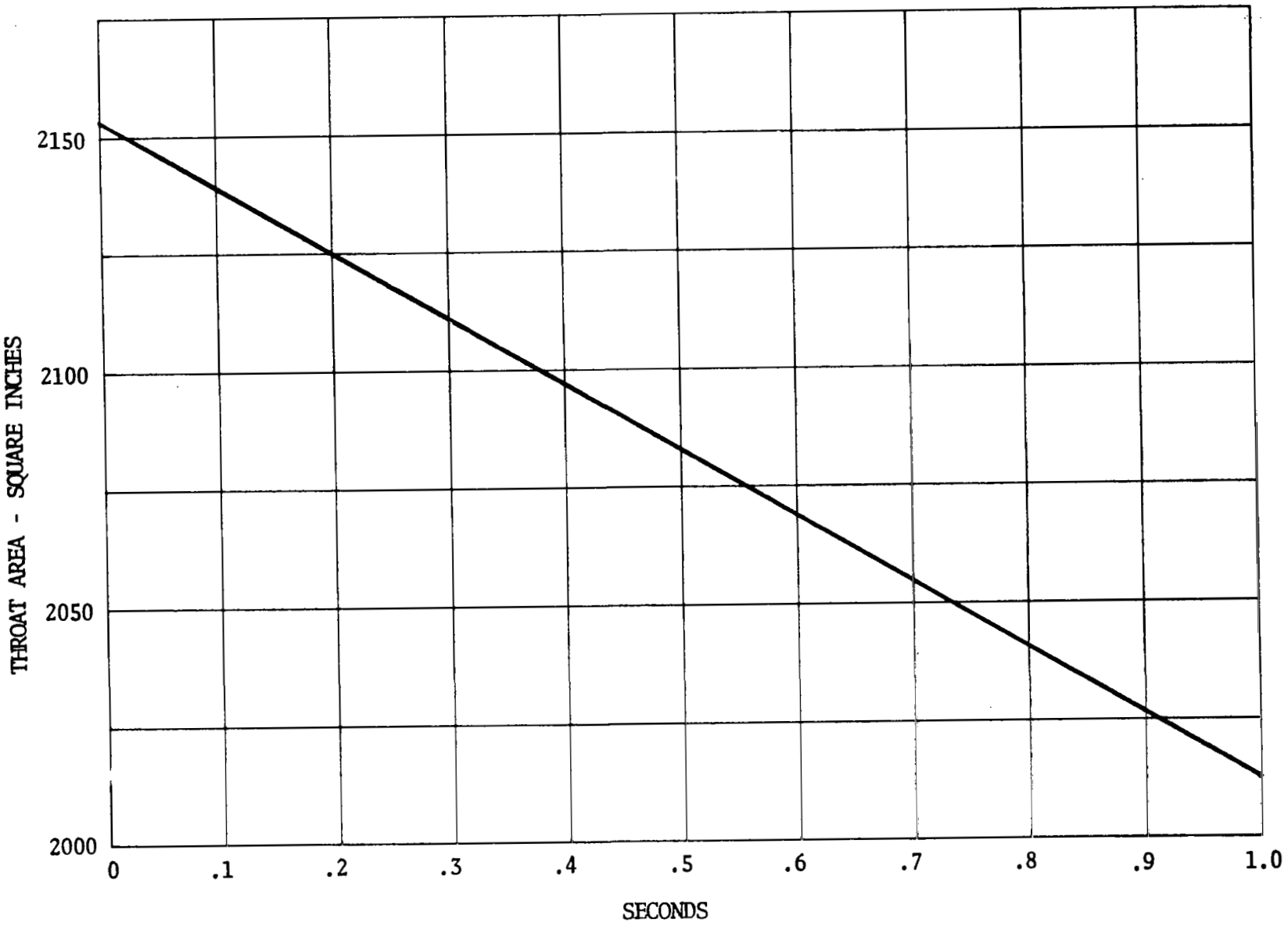

Figure 6. Simulation throat area schedule for throat-decreasing-induced unstart.

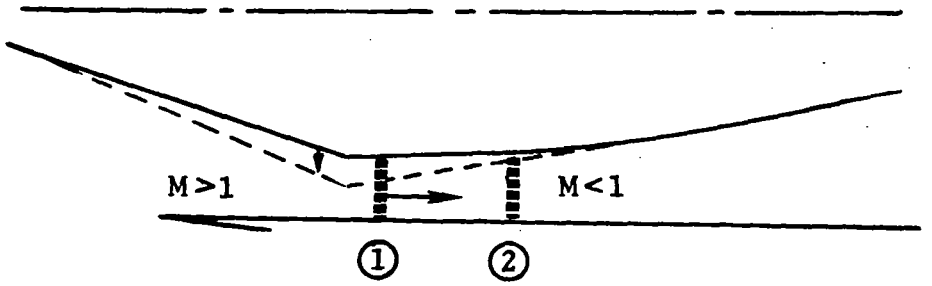

(a)

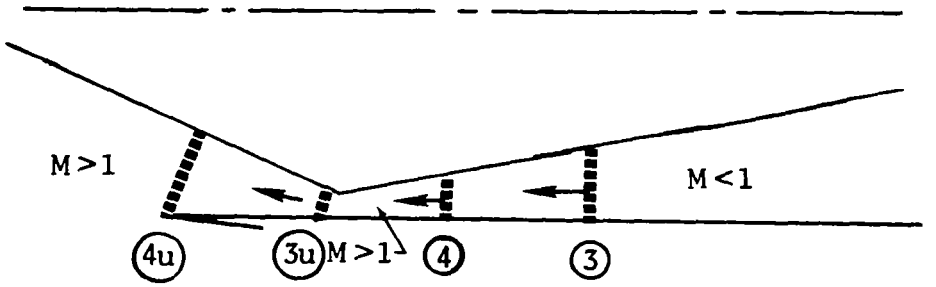

(b)

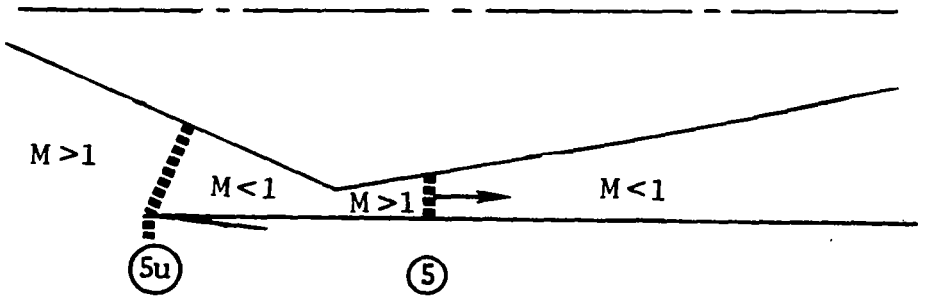

(c)

Figure 7. Conceptual diagrams of inlet operation during throat-decreasing-induced unstart.

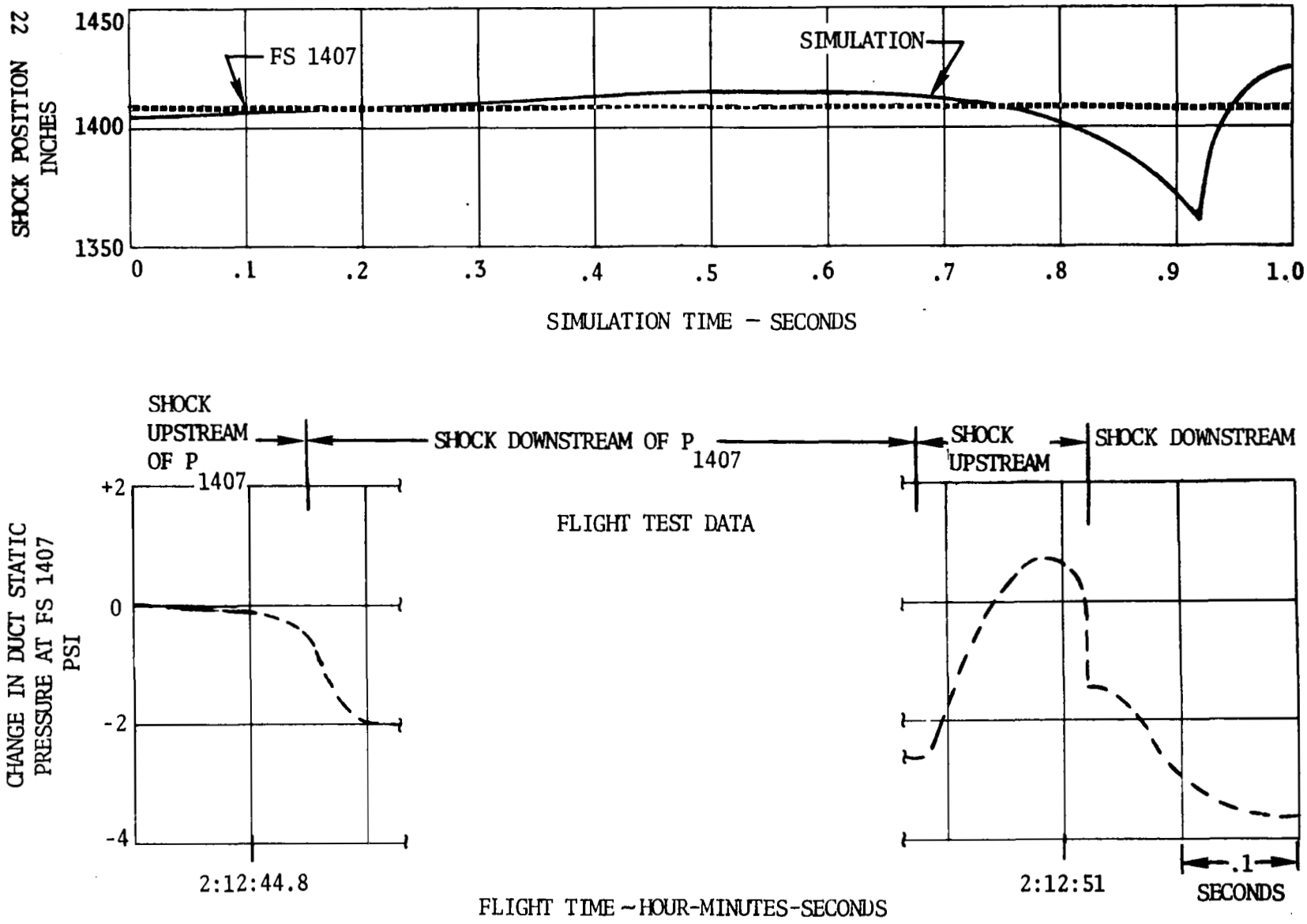

Figure 8. Correlation between flight measured duct static pressure change and simulation determined shock position during throat-decreasing-induced unstart.

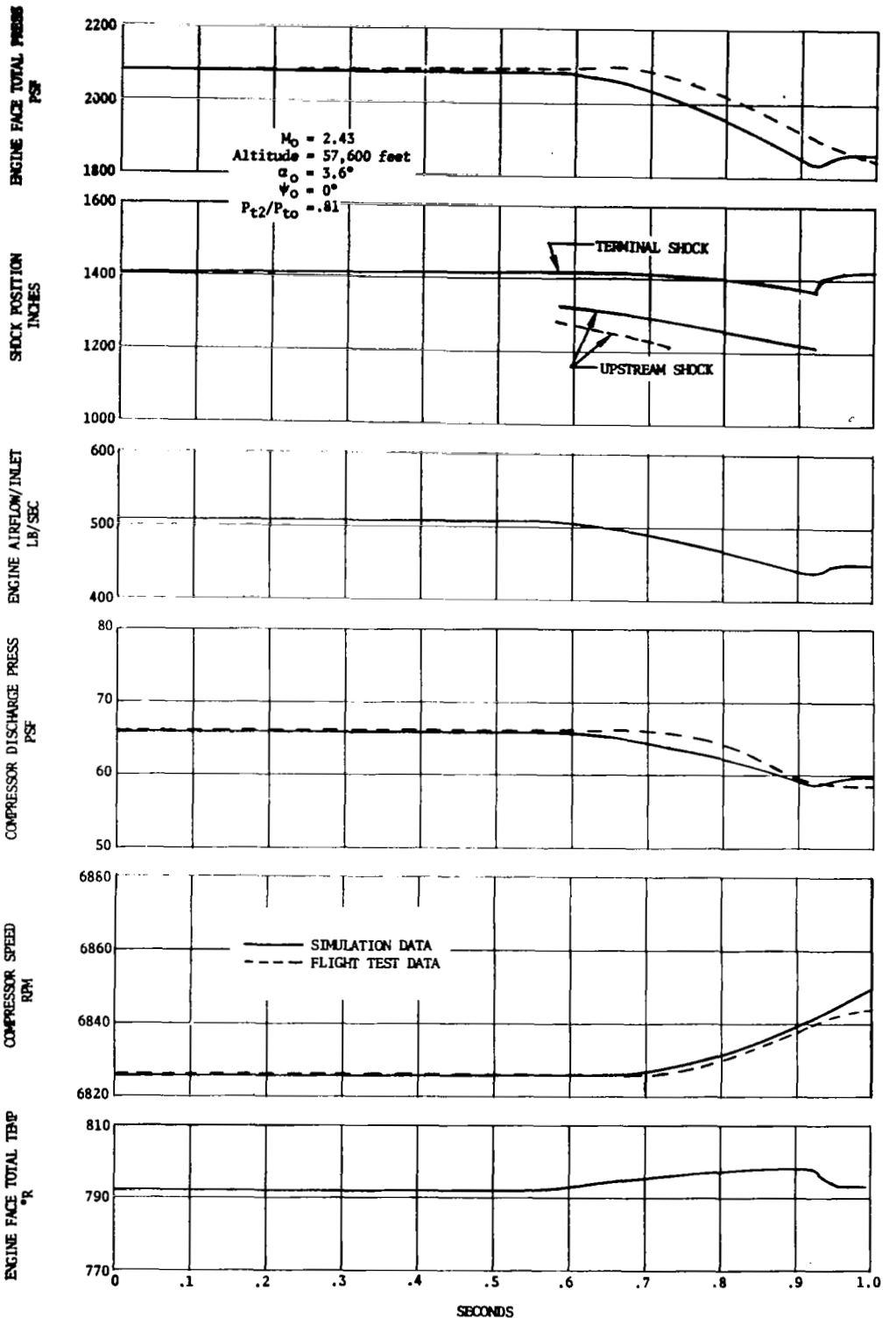

Figure 9. Comparison of flight test data and simulation data for throat-decreasing-induced unstart.

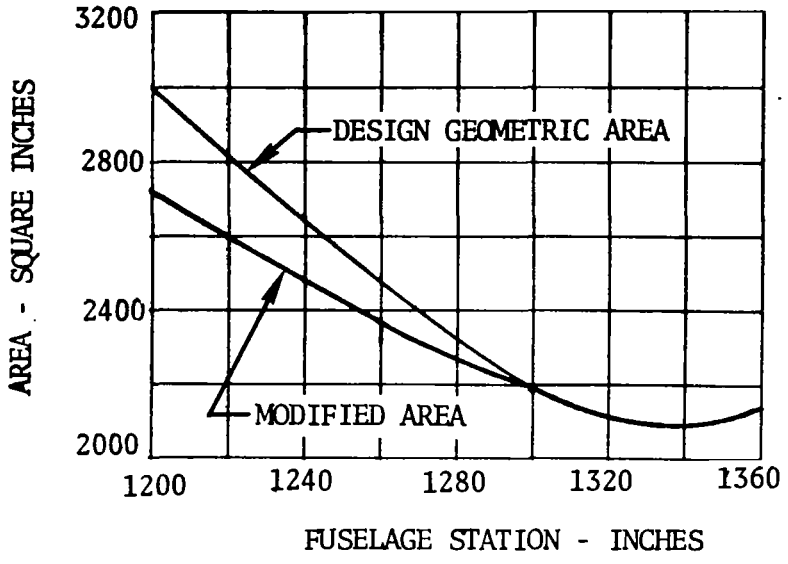

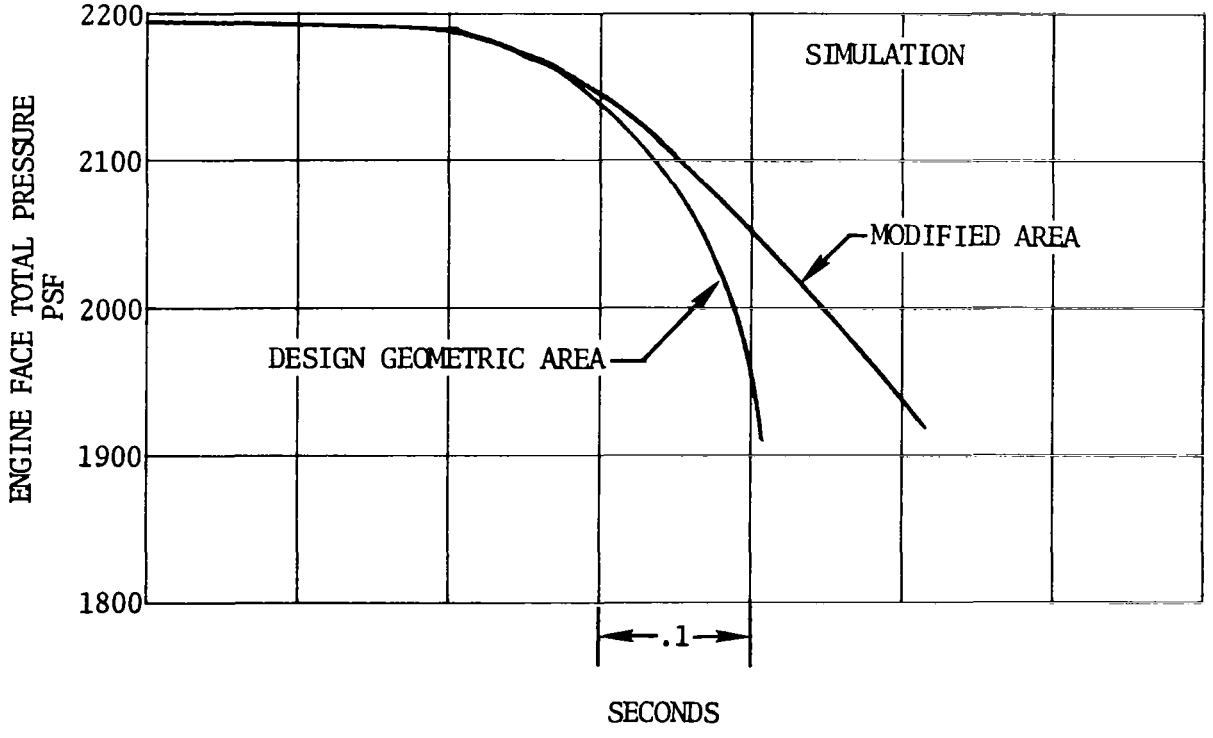

Figure 10. Engine face total pressures for two inlet configurations, throat-decreasing-induced unstart.

$M_o = 2.43$
Altitude = 50,080 feet
$\alpha_o = 3.7°$
$\psi_o = 0$
$P_{t2}/P_{to} = .88$

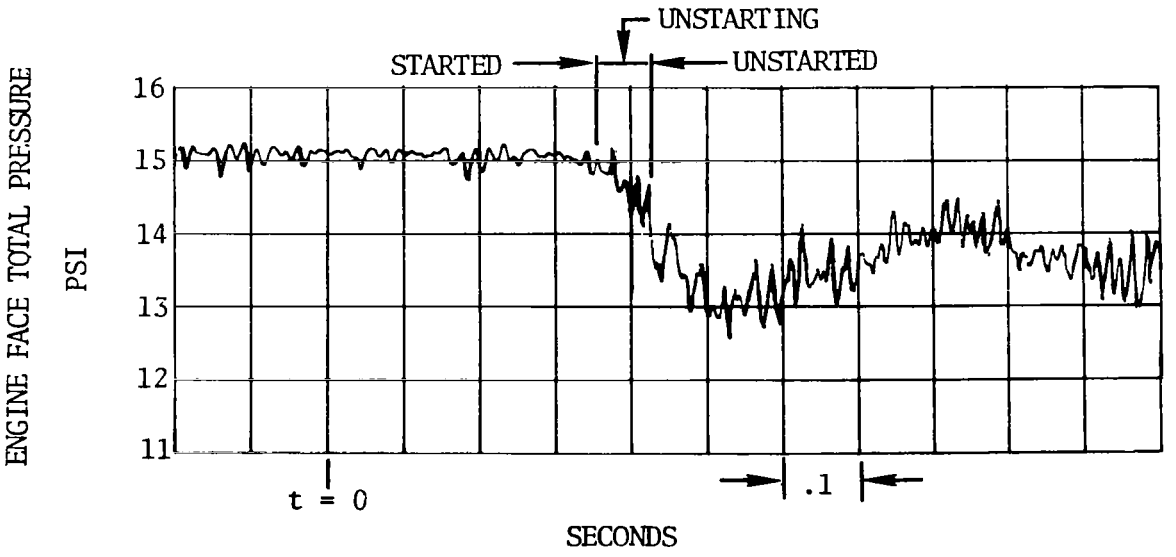

Figure 11. Flight test time history of engine face total pressure for throat-increasing-induced unstart.

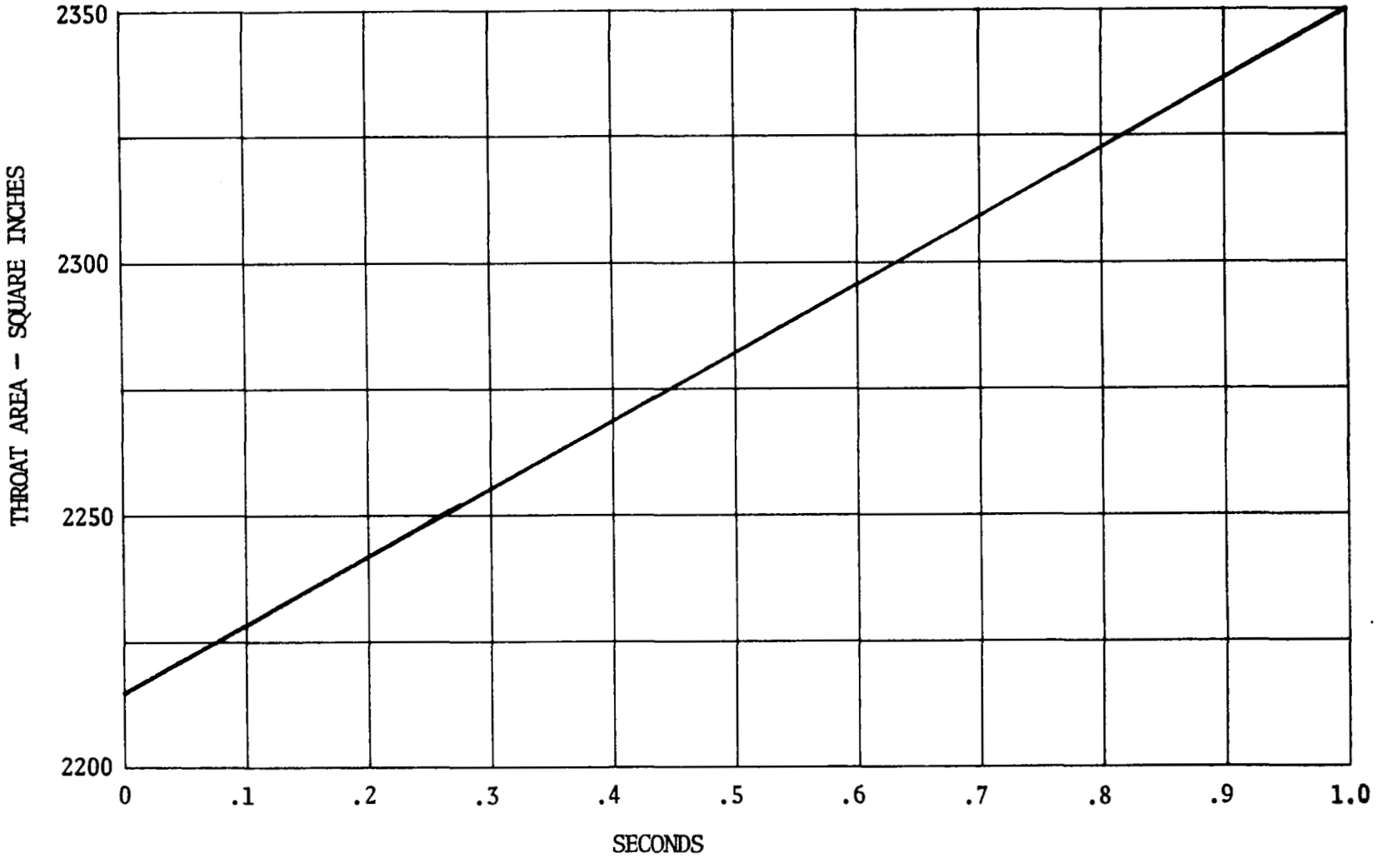

Figure 12. Throat area schedule for throat-increasing-induced unstart.

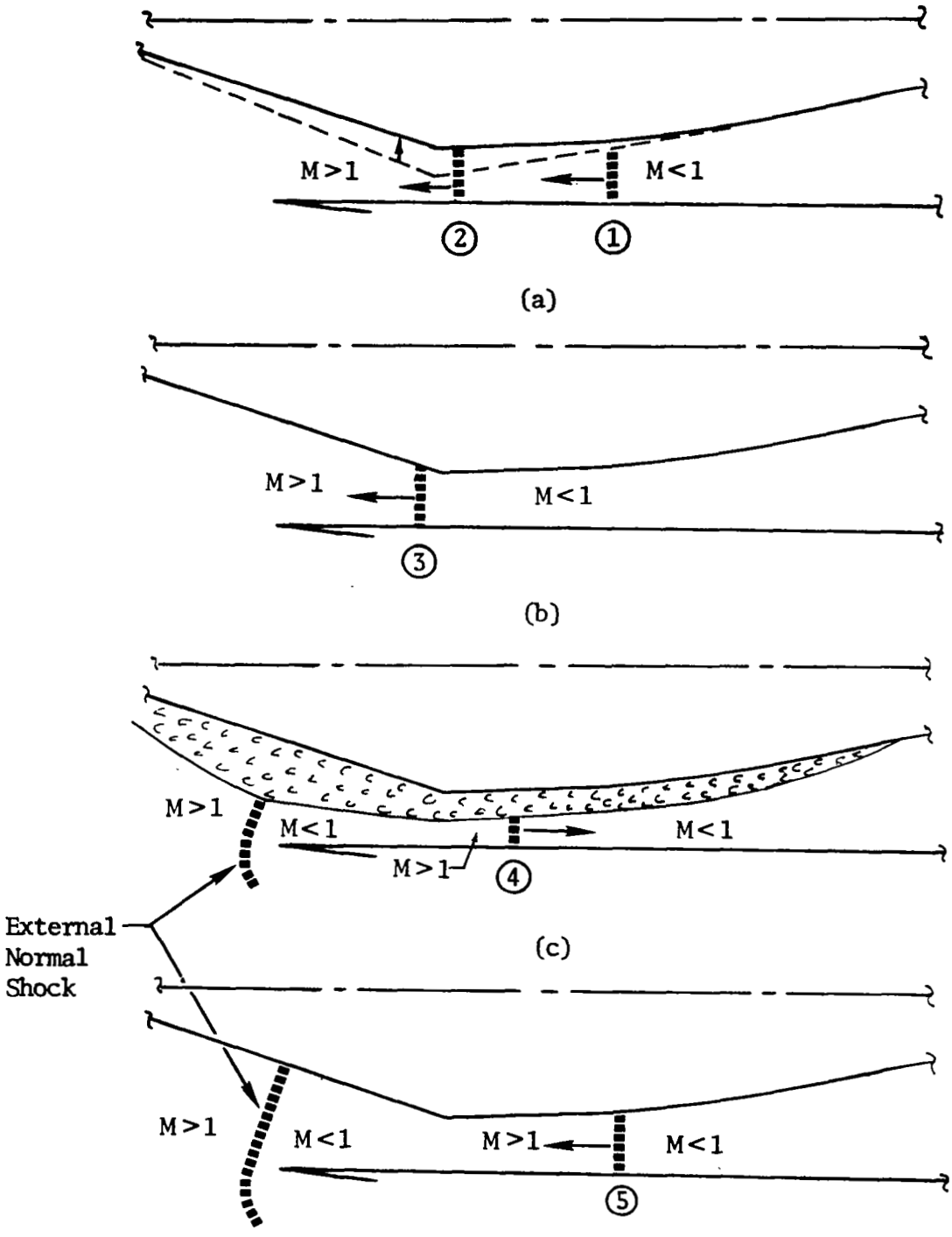

Figure 13. Conceptual diagrams of inlet operation during throat-increasing-induced unstarts.

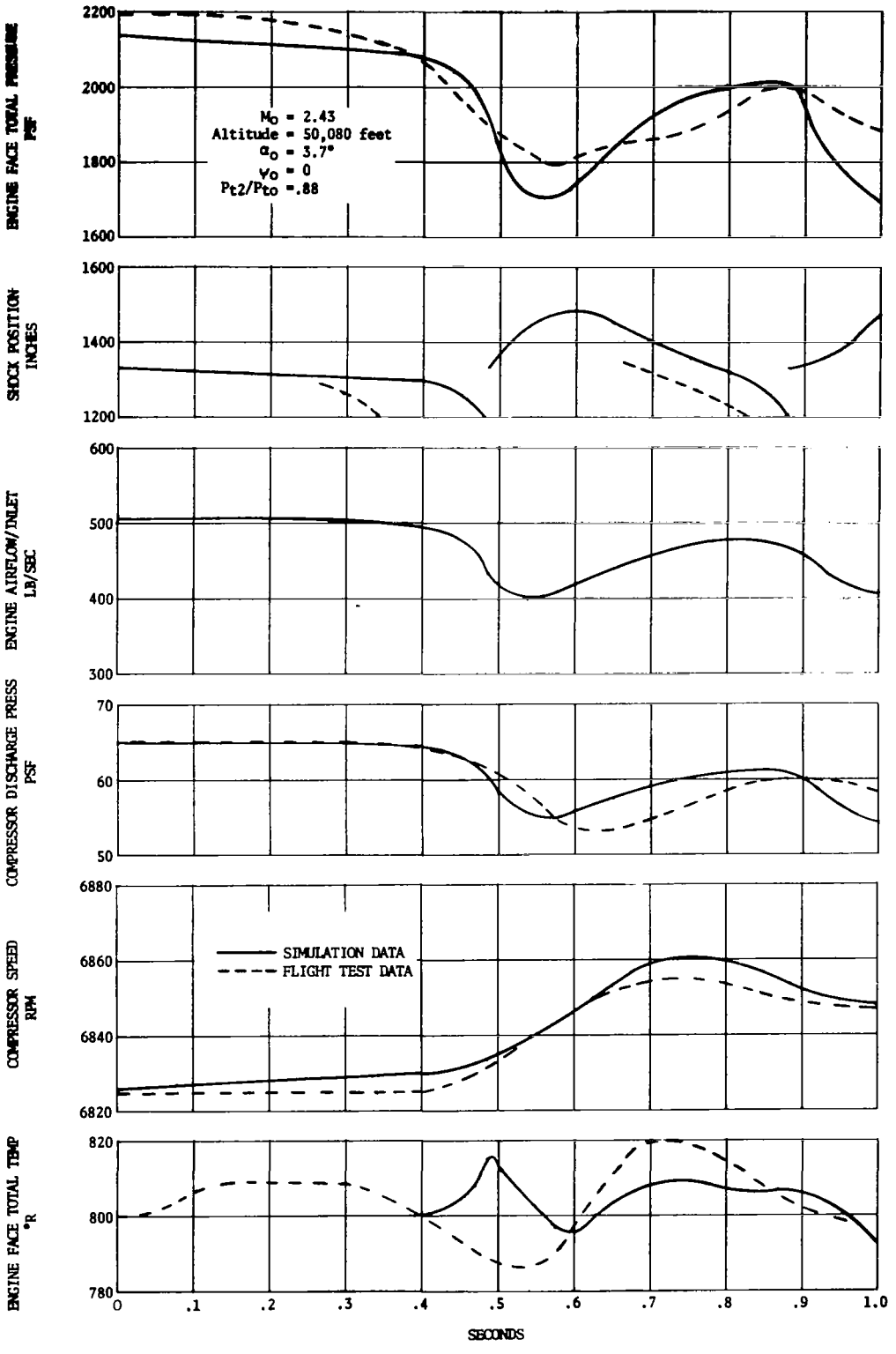

Figure 14. Comparison of flight test data and simulation data for throat-increasing-induced unstart.